Available online at www.sciencedirect.com
ScienceDirect
Developmental Biology 311 (2007) 500–511
DEVELOPMENTAL BIOLOGY
www.elsevier.com/developmentalbiology

Distinct and cooperative roles of mammalian Vg1 homologs GDF1 and GDF3 during early embryonic development

Olov Andersson *, Philippe Bertolino, Carlos F. Ibáñez *

Division of Molecular Neurobiology, Department of Neuroscience, Karolinska Institutet, S-17177 Stockholm, Sweden

Received for publication 30 March 2007; revised 18 August 2007; accepted 29 August 2007
Available online 14 September 2007

Abstract

Vg1, a member of the TGF-β superfamily of ligands, has been implicated in the induction of mesoderm, formation of primitive streak, and left–right patterning in *Xenopus* and chick embryos. In mice, GDF1 and GDF3 – two TGF-β superfamily ligands that share high sequence identity with Vg1 – have been shown to independently mimic distinct aspects of Vg1's functions. However, the extent to which the developmental processes controlled by GDF1 and GDF3 and the underlying signaling mechanisms are evolutionarily conserved remains unclear. Here we show that phylogenetic and genomic analyses indicate that *Gdf1* is the true *Vg1* ortholog in mammals. In addition, and similar to GDF1, we find that GDF3 signaling can be mediated by the type I receptor ALK4, type II receptors ActRIIA and ActRIIB, and the co-receptor Cripto to activate Smad-dependent reporter genes. When expressed in heterologous cells, the native forms of either GDF1 or GDF3 were incapable of inducing downstream signaling. This could be circumvented by using chimeric constructs carrying heterologous prodomains, or by co-expression with the Furin pro-protein convertase, indicating poor processing of the native GDF1 and GDF3 precursors. Unexpectedly, co-expression with Nodal – another TGF-β superfamily ligand involved in mesoderm formation – could also expose the activities of native GDF1 and GDF3, suggesting a potentially novel mode of cooperation between these ligands. Functional complementarity between GDF1 and GDF3 during embryonic development was investigated by analyzing genetic interactions between their corresponding genes. This analysis showed that $Gdf1^{-/-};Gdf3^{-/-}$ compound mutants are more severely affected than either $Gdf1^{-/-}$ or $Gdf3^{-/-}$ single mutants, with defects in the formation of anterior visceral endoderm and mesoderm that recapitulate Vg1 loss of function, suggesting that GDF1 and GDF3 together represent the functional mammalian homologs of Vg1.

Keywords: Growth and differentiation factors; tgf-b superfamily; Visceral endoderm; Nodal; Mesoderm; Gastrulation; Smad; Furin

Introduction

Signaling by members of the transforming growth factor beta (TGF-β) superfamily of ligands has been shown to regulate a number of important developmental processes, including cell differentiation, growth, and embryonic patterning (Heasman, 2006; Rossant and Tam, 2004; Shen, 2007; Tam et al., 2006). TGF-β ligands initiate signaling by assembling a heteromeric complex of type I and type II serine–threonine kinase receptors, in which the type II receptor phosphorylates the type I moiety. This results in the activation of the type I receptor and downstream signal transduction by phosphorylation of members of the Smad family of transcriptional regulators (Shi and Massague, 2003). The TGF-β superfamily of ligands includes more than 30 members, including the TGF-βs, Activins, Bone Morphogenetic Proteins, Growth and Differentiation Factors and Nodal. These ligands signal through specific combinations of 7 type I receptors, and 5 type II receptors. A large number of ligands converging on a smaller number of receptors raises the issues of signal fidelity and redundancy. From an evolutionary point of view, it could be favorable to have several ligands with redundant functions, and it has been argued that ligands evolve more readily than receptors (Sossin, 2006).

Ligands in the TGF-β superfamily are known to display overlapping functions during early development of frog and mouse embryos (Heasman, 2006; Shen, 2007). In *Xenopus*

* Corresponding authors.
E-mail addresses: olov.andersson@ki.se (O. Andersson), carlos.ibanez@ki.se (C.F. Ibáñez).

0012-1606/$ - see front matter © 2007 Elsevier Inc. All rights reserved.
doi:10.1016/j.ydbio.2007.08.060

laevis embryos, Vg1 has been implicated in activation of Smad2 and mesoderm formation. In particular, frog embryos treated with Vg1 antisense oligonucleotides lacked notochord, had fused somites along the midline, and reduced and abnormal neural structures (Birsoy et al., 2006; Joseph and Melton, 1998). Although it has been unclear whether a true Vg1 homolog is also present in the mouse, similar defects have been observed in hypomorphic mutants of the mouse gene *Nodal*, and in compound mutants between *Nodal* and *Gdf1* (growth and differentiation factor 1) (Andersson et al., 2006b; Lowe et al., 2001), suggesting possible evolutionary relationships between the signals that control those developmental processes.

Since mammalian GDF1 regulates left–right patterning in a similar way as Vg1 and shows high sequence similarity to this factor, GDF1 has been proposed to be the mammalian ortholog of amphibian Vg1 (Hyatt and Yost, 1998; Rankin et al., 2000; Wall et al., 2000). However, the GDF1 relative GDF3 has also been implicated in early embryonic development (Chen et al., 2006), and is structurally more closely related to both chick and amphibian Vg1 than GDF1 (see for example Fig. 1A). *Gdf3* mutant embryos have been found to display defects during formation of anterior visceral endoderm, mesoderm, and definitive endoderm with partial penetrance (Chen et al., 2006). Defects in the development of these structures have previously been described in *Nodal*, *Smad2* and *Cripto* mutants (Brennan et al., 2001; Ding et al., 1998; Norris et al., 2002; Vincent et al., 2003; Waldrip et al., 1998). GDF3 has also been shown to utilize the type I receptor ALK4, the type II receptor ActRIIB, and the co-receptor Cripto to activate downstream signaling (Chen et al., 2006), suggesting that it signals through the same receptors that have previously been demonstrated to mediate Nodal, GDF1 and Vg1 signaling (Cheng et al., 2003; Reissmann et al., 2001; Yeo and Whitman, 2001). Moreover, a recent study has indicated that GDF3 may function as a BMP inhibitor through the formation of GDF3/BMP4 heterodimers (Levine and Brivanlou, 2006).

The fact that *Gdf3* null mutants showed only a partially penetrant phenotype suggests the existence of other TGF-β ligands with redundant functions to GDF3. In particular, GDF1 could have partially redundant functions with GDF3 in the pre-gastrulation embryo, where both ligands have been shown to be expressed (Chen et al., 2006; Takaoka et al., 2006; Wall et al., 2000). In this study, we have examined the signaling capabilities of GDF3, and investigated the possible cooperation between GDF3 and GDF1 by generating and characterizing *Gdf1;Gdf3* compound mutant embryos.

Results

Comparison of Vg1, GDF1 and GDF3 protein sequences

A phylogenetic comparison of mouse TGF-β superfamily ligands with Vg1 sequences from *Xenopus laevis*, *Xenopus tropicalis*, and chicken shows that GDF1 and GDF3 form a subgroup of closely related molecules together with Vg1 proteins (Fig. 1A). Although the GDF3 precursor shares an overall higher amino acid identity with that of Vg1 than does

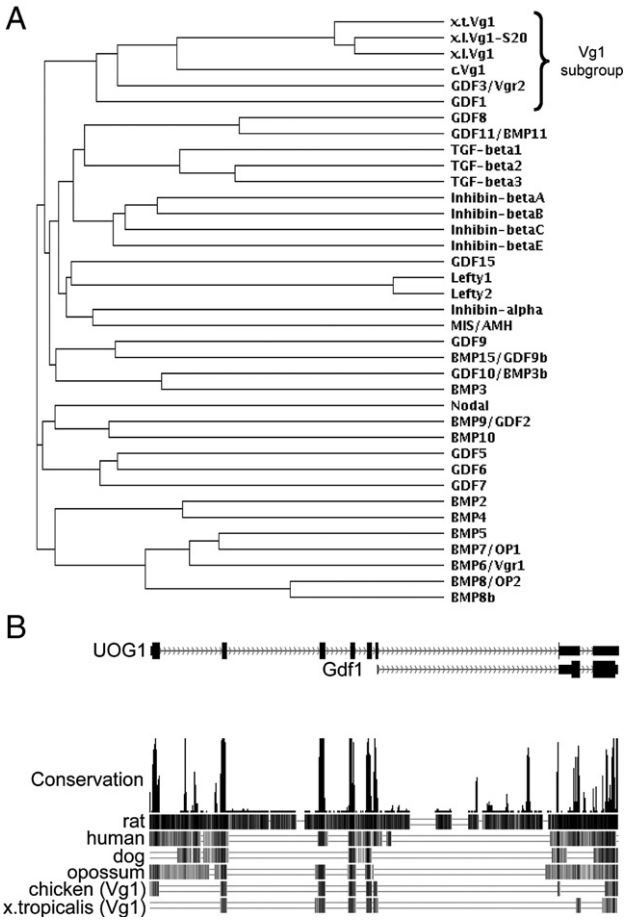

Fig. 1. Comparison of Vg1, GDF1, and GDF3 sequences. (A) Phylogenetic comparison of precursor protein sequences of TGF-β ligands found in mouse with Vg1 sequences from *Xenopus laevis*, *Xenopus tropicalis*, and chicken. Multiple sequence alignment was performed using ClustalW (Thompson et al., 1994). The second allele of *Vg1* that has recently been found in *Xenopus laevis* is termed Vg1-S20 (Birsoy et al., 2005). The Vg1 subgroup is indicated. (B) Alignment of the bicistronic *UOG-1/Gdf1* gene locus, including sequences from mammalian *Gdf1*, *Xenopus tropicalis Vg1*, and chicken *Vg1*. Schematic representations of the *UOG1* and *Gdf1* genomic loci from mouse are shown in the top, with exons indicated with dark boxes. Vertical black lines below indicate conserved sequences for each species, and the histogram shows the accumulated conservation. The assembly of sequences was performed using the UCSC Genome Browser.

GDF1 (38% vs. 30%, respectively), the mature sequences of GDF1 and GDF3 are equally related to that of Vg1 (58% and 57% amino acid identity, respectively). Interestingly, GDF3 also shares 6 out of 7 amino acids with GDF1 and Vg1 in the C-terminal β8-subregion, which has been shown to be critical for signaling through the Cripto co-receptor (Cheng et al., 2004). Thus, phylogenetic analyses support either GDF1 or GDF3 as the mammalian ortholog of Vg1, and suggest they use similar signaling mechanisms.

The mouse *Gdf1* gene has an unusual structure in which the transcript encoding GDF1 can either be produced alone or as a bicistronic mRNA together with an upstream open reading frame (Lee, 1991). Interestingly, the sequence upstream of *Gdf1* (UOG-1) has a conserved pattern that cannot be found upstream of *Gdf3*. By aligning genomic sequences from several

mammalian species with genomic regions corresponding to the *Vg1* gene from *Xenopus tropicalis* and chicken, we found that this bicistronic gene structure, as well as other genes in the region, are also conserved in the vicinity of frog and chicken *Vg1* (Fig. 1B). Although no such genomic sequences are available from *Xenopus laevis*, the close relationship between *laevis* and *tropicalis* suggests that this structure should also be present in *laevis*. Thus, together, phylogenetic and genomic analyses suggest *Gdf1*, but not *Gdf3*, is the true mammalian ortholog of *Vg1*. We are currently unable to find any sequences that could correspond to *Xenopus* or chicken *Gdf3*, although at present only half of the *Xenopus tropicalis* genome has been completed. *Gdf3* could thus have arisen from a recent gene duplication in the mammalian clade, and *Vg1* be a pro-ortholog to *Gdf1* and *Gdf3*. The expression of GDF1 and GDF3 in the embryonic ectoderm suggest that their combined functions in the developing mouse embryo may together represent those of Vg1 in the frog.

Processed GDF1 and GDF3 signal in a Cripto-dependent fashion

The close sequence identity between GDF1 and GDF3 suggests that they may signal in a similar fashion. GDF1 has previously been shown to require the co-receptor Cripto in order to signal through the type I receptor ALK4 and the type II receptor ActRIIB (Cheng et al., 2003). GDF1 can also signal through ALK7, although its effects during embryogenesis seem to be mediated via ALK4 (Andersson et al., 2006b). Studies of GDF1 signaling have been hampered by poor processing of the native precursor protein. This is a feature that GDF1 appears to share with GDF3 and Vg1 (Chen et al., 2006). One way to circumvent this problem is to produce these ligands as chimeric proteins with prodomains from other family members that are more easily processed. We therefore generated chimeric proteins in which the mature domain of GDF3 was positioned downstream of either *Xenopus* Activin B or BMP2 prodomains. We subsequently analyzed their activities in comparison with that of native GDF3 and other TGF-β superfamily ligands. HepG2 cells were transfected with the Smad3-dependent luciferase reporter CAGA-Luc (Dennler et al., 1998) together with increasing doses of expression constructs of various ligands in the presence or absence of Cripto (Fig. 2A).

A chimeric protein consisting of a *Xenopus* BMP2 pro-domain and a GDF11 mature-domain (B/GDF11), used as a positive control, activated the reporter in a dose-dependent fashion in the absence of Cripto, as previously documented (Andersson et al., 2006a). Without Cripto expression, none of the other ligands tested had any effect in these conditions. Another control utilized, a chimeric protein of *Xenopus* Activin B pro-domain and the mature domain of *Xenopus* Nodal related 1 (A/Xnr1), activated the reporter only in the presence of Cripto

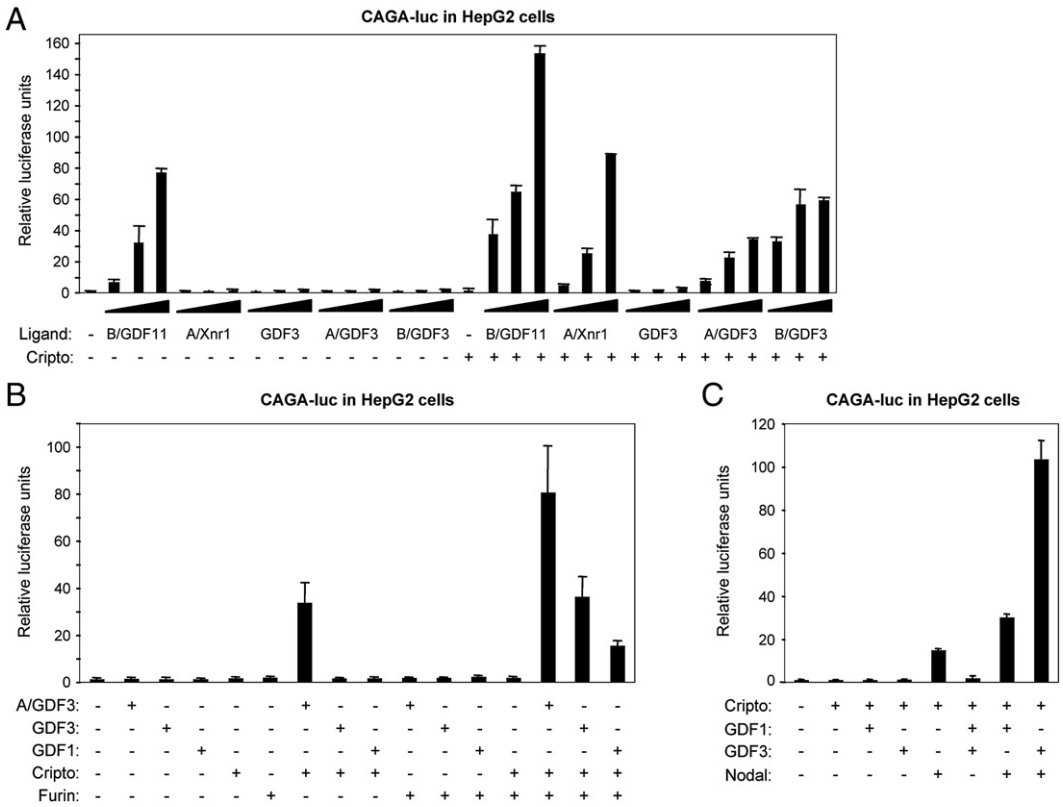

Fig. 2. GDF1 and GDF3 signal in a Cripto-dependent fashion. (A) HepG2 cells were transfected with a CAGA-luc reporter construct and increasing doses (50, 200, and 800 ng) of plasmids encoding different ligands in the presence or absence of Cripto. (B) HepG2 cells transfected with a CAGA-luc reporter and 200 ng of plasmids encoding native GDF1, native GDF3 or chimeric A/GDF3 in the presence or absence of Cripto and a plasmid carrying the pro-protein convertase Furin. (C) HepG2 cells transfected with CAGA-luc reporter, 200 ng plasmids encoding native ligands, and Cripto. The ligands were transfected alone and in different combinations to allow assessment of their synergistic effects.

as expected (Cheng et al., 2003; Reissmann et al., 2001; Yeo and Whitman, 2001). Interestingly, although GDF11 signaling was in principle Cripto independent, its activity could be potentiated by Cripto overexpression (Fig. 2A), suggesting some level of interaction between these two proteins. In the presence of Cripto, native GDF3 could only very weakly activate the reporter (about 2-fold over baseline) at the highest dose tested, in agreement with previous findings (Chen et al., 2006). However, when the mature domain of GDF3 was linked to the prodomains of either *Xenopus* Activin B (A/GDF3) or *Xenopus* BMP2 (B/GDF3), a strong dose-dependent activation of the reporter could be detected in the presence, but not in the absence, of Cripto (Fig. 2A). We conclude that both chimeric constructs of GDF3 can mimic Nodal signaling when co-expressed with the Cripto co-receptor.

We hypothesized that native GDF3 protein may be poorly processed in this cell line due to inadequate levels of pro-protein convertases. We therefore co-expressed either native GDF3, native GDF1 or the chimeric protein A/GDF3 with the pro-protein convertase Furin and tested their activities in the reporter assay (Fig. 2B). The activity of all three constructs was significantly increased in the presence of Furin. Potentiation was most significant in the case of native GDF3 (Fig. 2B).

Finally, and because GDF1 and GDF3 appear to be co-expressed with Nodal at several developmental stages – albeit not always (see Discussion), the possibility that their activities may in some way be influenced by Nodal was also investigated. To this purpose, constructs carrying either native GDF1 or GDF3 sequences were co-expressed together with native Nodal and Cripto and tested for activation of the CAGA-Luc reporter in HepG2 cells. As expected, native Nodal readily activated the Smad3 reporter (≈ 15-fold), while no activity could be detected with either native GDF1 or GDF3 at the doses tested (Fig. 2C). However, both GDF1 and GDF3 could potentiate Nodal activity in a synergistic manner (by 2- and 7-fold, respectively), indicating that Nodal co-expression can uncover the intrinsic activity of native GDF1 and GDF3 proteins. Co-expression of GDF1 and GDF3 in the absence of Nodal did not result in any significant activation of the reporter (Fig. 2C). We conclude that both GDF1 and GDF3 can signal via Smad3 in a Cripto-dependent fashion when efficiently processed or if co-expressed with Nodal.

Characterization of GDF3 signaling through type I and type II receptors

Next, we extended the reporter assay analysis to examine the ability of GDF3 to signal via distinct type I and type II receptors. For these experiments, we utilized R4-2 cells, a cell-line expressing low levels of endogenous type I receptors and thus better suited for reconstitution experiments. We found that activation of the reporter by A/GDF3 required co-expression of the Activin type I receptor ALK4, but not the TGF-β type I receptor ALK5, and that signaling strength was potentiated by co-expression of Cripto (Fig. 3A). In this cell line, however, the dynamic range of the response appeared to be limited by background activity, most likely due to endogenous production of ligand or other signaling components. In order to obtain independent measurements circumventing this problem, we generated a chimeric receptor in which the L45-loop of ALK4

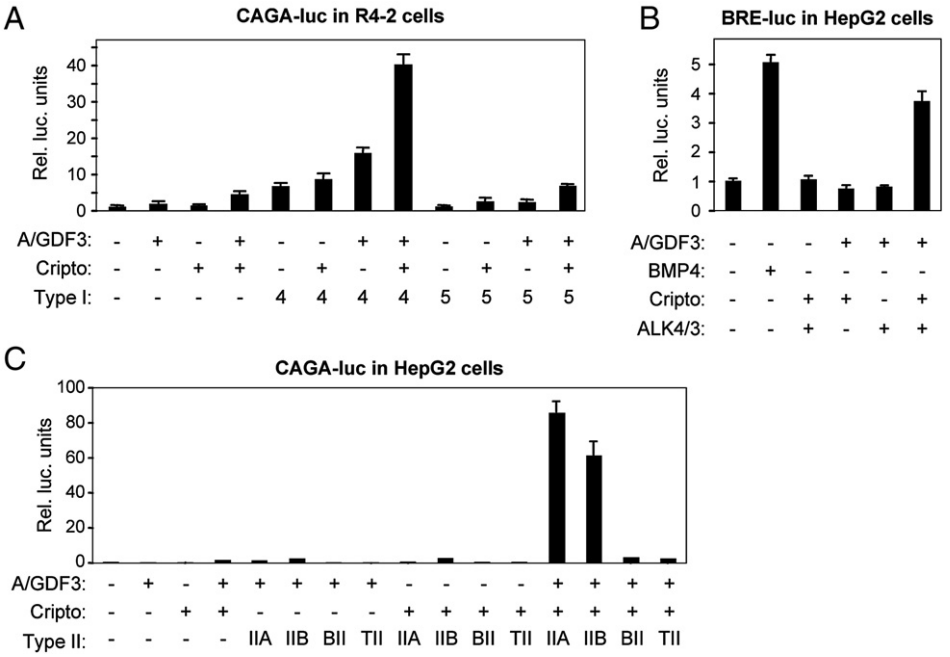

Fig. 3. GDF3 signaling through type I receptor ALK4 and type II receptors ActRIIA and ActRIIB. (A) R4-2 cells transfected with a CAGA-luc reporter and plasmids encoding A/GDF3, and the type I receptors ALK4 and ALK5 in the presence or absence of Cripto. (B) HepG2 cells transfected with a BRE-luc reporter and plasmids encoding A/GDF3, Cripto, and chimeric type I receptor ALK4/3. 50 ng/ml of BMP4 protein was used as a positive control for reporter activation. (C) HepG2 cells transfected with CAGA-luc reporter and plasmids encoding A/GDF3, Cripto, and type II receptors. IIA, ActRIIA; IIB, ActRIIB; TII, TGF-β type II receptor; BII, BMP type II receptor.

was replaced with the corresponding sequence from the BMP receptor ALK3, herein referred to as the ALK4/3 receptor chimera. The L45 loop of the type I receptor interacts with Smad proteins and determines the Smad specificity for the receptor (Chen et al., 1998; Persson et al., 1998). The chimeric receptor was expressed in HepG2 cells together with a reporter construct containing a BMP responsive element (BRE) from the *xVent* promoter upstream of a luciferase gene BRE-Luc (Hata et al., 2000). Using this assay, we found that A/GDF3 could significantly activate the reporter only in the presence of the ALK4/3 chimeric receptor co-expressed with Cripto (Fig. 3B). Taken together, these results indicate that GDF3 can signal through ALK4 in a Cripto-dependent fashion.

In order to examine which type II receptors mediate GDF3 signaling, we used HepG2 cells which express high levels of endogenous type I receptors, and are very sensitive to addition of type II receptors. Reporter gene activity was greatly enhanced when either ActRIIA or ActRIIB were co-expressed with A/GDF3 and Cripto, but it was not significantly activated by addition of the BMP type II receptor nor the TGF-β type II receptor (Fig. 3C). We conclude that GDF3 signals through the type II receptors ActRIIA and ActRIIB to activate a Smad3-dependent reporter.

Genetic interaction between Gdf1 and Gdf3

In order to explore physiological functions of GDF3 during early development, we generated *Gdf3* mutant mice from ES cells carrying a gene trap in the single intron of *Gdf3* (obtained from the Sanger Institute) (Fig. 4A). Approximately 50% of mice homozygous for the gene trap insertion survived until adulthood and were fertile. No *Gdf3* mRNA could be detected by RT–PCR in embryos or adult tissues from *Gdf3* mutant mice (Fig. 4B), indicating that the gene trap is likely to represent a null allele. An initial screen of embryos obtained from interbreeding of $Gdf3^{+/-}$ animals revealed variable phenotypes in a subset of $Gdf3^{-/-}$ mutants at embryonic day 8.5 (E8.5). Affected embryos displayed either anterior truncations or more severe defects affecting the body plan (Fig. 4C). At this stage, we also frequently found empty yolk sacs and resorbed embryos that were not possible to genotype, which together indicated an early phenotype in agreement with previous findings (Chen et al., 2006).

GDF3 has previously been found to contribute to the formation of the primitive streak, mesoderm and anterior visceral endoderm (AVE), as well as the migration of the AVE from the distal tip to the prospective anterior side of the epiblast (Chen et al., 2006). In view of their structural similarities, their common relationship to Vg1, and their overlapping expression in the embryonic ectoderm at pre-gastrulation stages, it is possible that GDF1 and GDF3 together contribute to those functions (Chen et al., 2006; Takaoka et al., 2006; Wall et al., 2000). We set out to test this notion by examining whether deletion of *Gdf1* can augment the phenotypes found in $Gdf3^{-/-}$ mutants. To this end, we generated $Gdf1^{-/-};Gdf3^{-/-}$ double null mutants by intercrossing $Gdf1^{+/-};Gdf3^{+/-}$ double heterozygous mice.

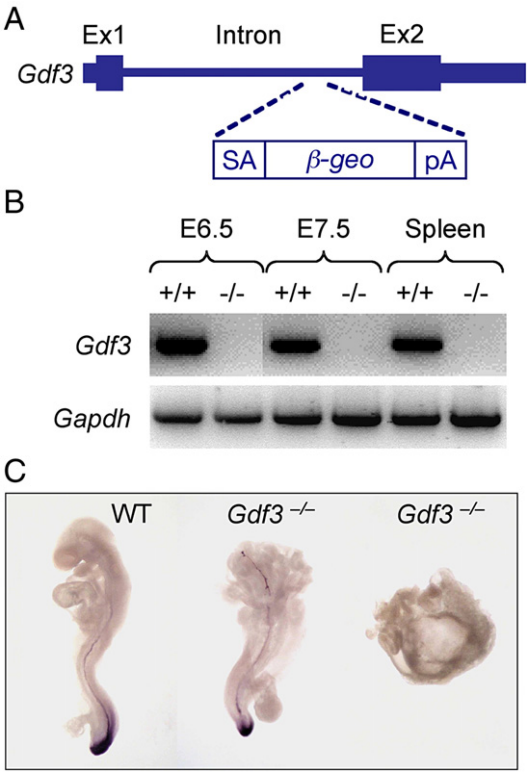

Fig. 4. Generation of *Gdf3* mutant mice. (A) Schematic illustration of the gene trap insertion in the *Gdf3* gene. The gene trap contains a splice acceptor (SA) followed by a fusion of β-galactosidase and neomycin transferase (*β-geo*), and a SV40 polyadenylation signal (pA). The gene trap insertion was localized to the first intron of the *Gdf3* gene by PCR, using 24 different primer combinations spanning different regions of this intron. (B) *Gdf3* expression was analyzed by RT–PCR in wild type and $Gdf3^{-/-}$ mutant embryos and in adult spleen. No *Gdf3* mRNA expression could be detected in homozygous mutants. (C) *T* expression in wild-type (WT) and two differently affected $Gdf3^{-/-}$ E8.5 mutant embryos analyzed by whole-mount *in situ* hybridization.

Double null mutants were found at expected Mendelian frequencies between E6.25 and E6.75 ($n=178$). However, 1/6 of *Gdf3* null embryos were lost at E7.5 and E8.5 ($n=125$, and $n=120$, respectively), indicating some embryonic lethality in $Gdf3^{-/-}$ mutants as indicated above. The under-representation of homozygous *Gdf3* mutants at those stages did not correlate with the status of the *Gdf1* allele, although it was clear that the severity of the phenotypes observed in these embryos was augmented in both $Gdf1^{+/-};Gdf3^{-/-}$ and $Gdf1^{-/-};Gdf3^{-/-}$ compound mutants when compared to $Gdf3^{-/-}$ single mutant littermates (see below). $Gdf1^{-/-}$ single mutants, $Gdf1^{+/-};Gdf3^{+/-}$ double heterozygous and $Gdf1^{-/-};Gdf3^{+/-}$ compound mutants appeared to develop normally. In addition to double heterozygous intercrosses, $Gdf1^{-/-};Gdf3^{-/-}$ double mutant embryos were also obtained by interbreeding $Gdf1^{+/-};Gdf3^{-/-}$ mutants.

GDF1 and GDF3 cooperate during formation of the anterior visceral endoderm (AVE) and establishment of anterior–posterior identity

The AVE is an extra-embryonic cell population that is induced at the distal region of the epiblast and subsequently

migrates upwards to the prospective anterior side of the pre-gastrulation embryo. At the onset of gastrulation, the AVE promotes expression of forebrain markers in the anterior region of the epiblast. Lack of AVE has previously been associated with anterior truncations that resemble those observed at E8.5 in *Gdf3*$^{-/-}$ mutants (Fig. 4C).

In order to shed light on the mechanisms underlying the defects observed in single and double mutants of *Gdf1* and *Gdf3*, we analyzed compound mutants by whole-mount *in situ* hybridization with probes specific to *Lefty1*, *Brachyury* (herein denoted as *T*), *Nodal*, and *Otx2*, which serve as markers for AVE, mesoderm, posterior epiblast and anterior neuroectoderm, respectively. At E6.5, the AVE has normally migrated to the anterior side of the epiblast (Fig. 5A). We found two distinct phenotypes differing in severity among the mutants, one in which the AVE was induced distally but did not migrate to the anterior side (herein referred to as type I), and another in which the AVE was totally absent (herein referred to as type II). All affected embryos carried a homozygous null mutation in *Gdf3* and both the incidence and severity of the defects increased with a homozygous null mutation in *Gdf1*. Mutations in *Gdf1* were on their own insufficient to generate those defects. Approximately 50% of *Gdf1*$^{+/+}$;*Gdf3*$^{-/-}$ or *Gdf1*$^{+/-}$;*Gdf3*$^{-/-}$ embryos displayed either type I or type II defects, whereas 83% of *Gdf1*$^{-/-}$;*Gdf3*$^{-/-}$ mutants were affected (Fig. 5A). The severity of the defects observed also increased in *Gdf1*$^{-/-}$;*Gdf3*$^{-/-}$ mutants, such that 58% displayed type II defects, compared to 20% in *Gdf1*$^{+/+}$;*Gdf3*$^{-/-}$ or *Gdf1*$^{+/-}$;*Gdf3*$^{-/-}$ mutants. Thus, these results indicate that GDF1 and GDF3 cooperate during formation of the AVE.

Synergistic interactions between *Gdf1* and *Gdf3* genes were investigated further by looking at the expression of mesodermal markers in *Gdf1*$^{-/-}$;*Gdf3*$^{-/-}$ compound mutants. Ectopic expression of mesodermal markers has been observed at the onset of gastrulation in null mutants for various components of the Nodal pathway, such as *Smad2* and *Foxh1* (Waldrip et al., 1998; Yamamoto et al., 2001). We found ectopic expression of

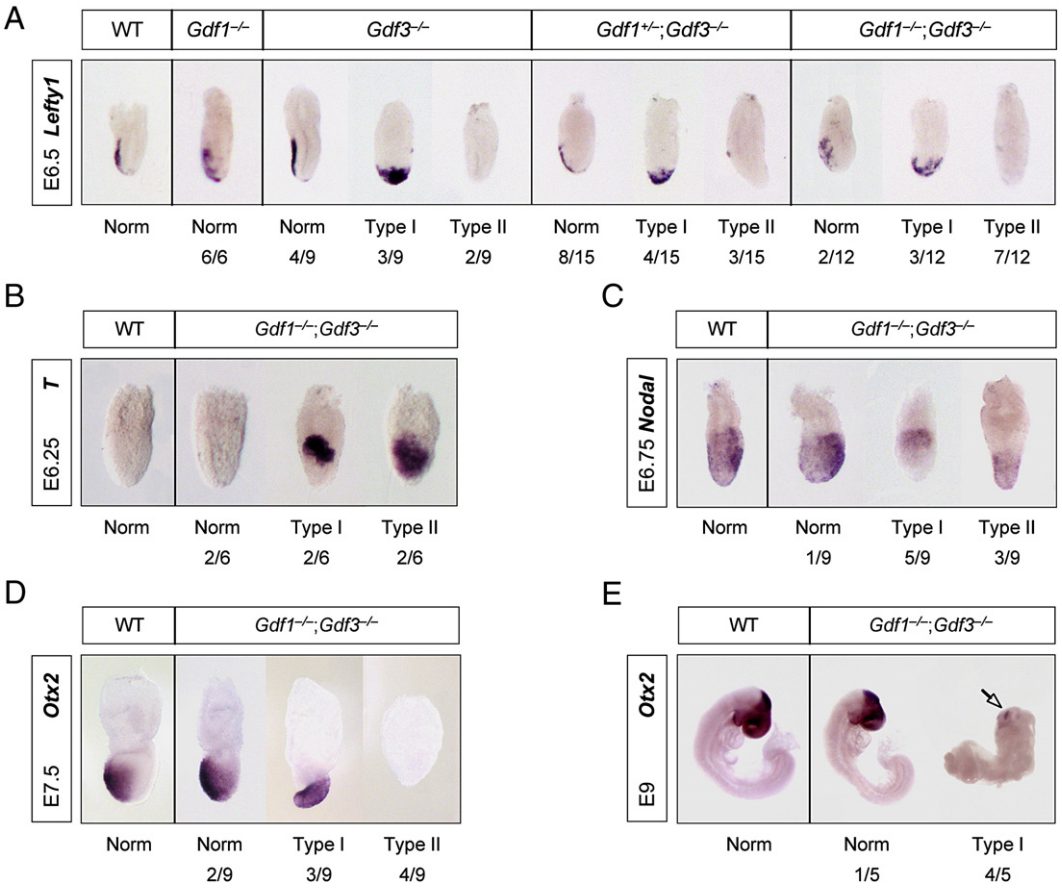

Fig. 5. GDF1 and GDF3 cooperate during formation of anterior visceral endoderm and initiation of gastrulation. (A) Expression of *Lefty1* in AVE of E6.5 wild type, *Gdf1*$^{-/-}$ and *Gdf3*$^{-/-}$ single mutants, and *Gdf1*$^{+/-}$;*Gdf3*$^{-/-}$ and *Gdf1*$^{-/-}$;*Gdf3*$^{-/-}$ compound mutant embryos. Several embryos of the same genotype are shown when variable phenotypes occurred. Phenotypes were grouped into different classes (normal, type I and type II) as explained in the text. The frequency of each phenotype within a given genotype is indicated. (B) Expression of *T* in the epiblast in E6.25 wild type and *Gdf1*$^{-/-}$;*Gdf3*$^{-/-}$ compound mutants. Ectopic expression of *T* is restricted to the proximal embryonic ectoderm (Type I), or else found throughout the epiblast (Type II) in affected compound mutant embryos. (C) Expression of *Nodal* in E6.75 wild type and *Gdf1*$^{-/-}$;*Gdf3*$^{-/-}$ compound mutants. *Nodal* is normally expressed in the posterior epiblast of wild type embryos (Norm), but appeared either proximally (Type I), or distally (Type II) in affected *Gdf1*$^{-/-}$;*Gdf3*$^{-/-}$ mutants. (D) Expression of *Otx2* in E7.5 wild type and *Gdf1*$^{-/-}$;*Gdf3*$^{-/-}$ compound mutants. *Otx2* is normally expressed in the anterior neuroectoderm in wild type embryos (Norm), but was found uniformly expressed (Type I), or else absent (Type II) in affected *Gdf1*$^{-/-}$;*Gdf3*$^{-/-}$ mutants. (E) Expression of *Otx2* in E9 wild type and *Gdf1*$^{-/-}$;*Gdf3*$^{-/-}$ compound mutants. *Otx2* is normally expressed in forebrain and midbrain territories (Norm), but its expression domain was severely reduced in anteriorly truncated embryos (Type I). Arrow indicates *Otx2* expression. Empty yolk sacs, found at this stage, most likely correspond to type II affected embryos (not shown).

T in either the proximal embryonic ectoderm or throughout the whole epiblast in 67% of *Gdf1*$^{-/-}$;*Gdf3*$^{-/-}$ mutants prior to gastrulation (referred to as a type I and II defects in Fig. 5B, respectively). Expression of *Nodal* is normally restricted to the posterior side of the epiblast. We found abnormal *Nodal* expression in the proximal epiblast (type I) or the visceral endoderm (type II) in 55% and 33%, respectively, of *Gdf1*$^{-/-}$;*Gdf3*$^{-/-}$ embryos at E6.75 (Fig. 5C).

The AVE promotes forebrain markers, such as *Otx2*, in the embryonic ectoderm on the anterior side of the epiblast. Analysis of *Otx2* expression at E7.5 revealed two distinct phenotypes in *Gdf1*$^{-/-}$;*Gdf3*$^{-/-}$ compound mutants that differed in severity. *Otx2* transcripts were either found in a uniform distal location, or else totally absent in an otherwise very small and disorganized embryo (referred to as a type I and II in Fig. 5D, respectively). At E9, *Otx2* expression was weak and restricted to a small patch of cells in the anterior region of surviving *Gdf1*$^{-/-}$;*Gdf3*$^{-/-}$ embryos (Fig. 5E). Together, these findings indicate that *Gdf1* and *Gdf3* have partially redundant functions during formation of the anterior–posterior axis, and that *Gdf1* can to some extent compensate for the absence of *Gdf3*.

Mutation of Gdf1 and Gdf3 leads to defects in mesoderm formation

Next, we examined the formation of mesoderm in E7.5 compound mutants in greater detail, using markers for primitive streak and axial mesoderm (*T*), and anterior primitive streak and axial mesoderm (*FoxA2*). Genetic interaction between *Gdf1* and *Gdf3* resulted in similar gene–dosage effects at E7.5 as those observed at E6.5. Analysis of *T* expression at E7.5 revealed one set of double-mutant embryos that, although able to form mesoderm, showed abnormalities in primitive streak elongation (Fig. 6A). We refer to E7.5 embryos displaying this phenotype

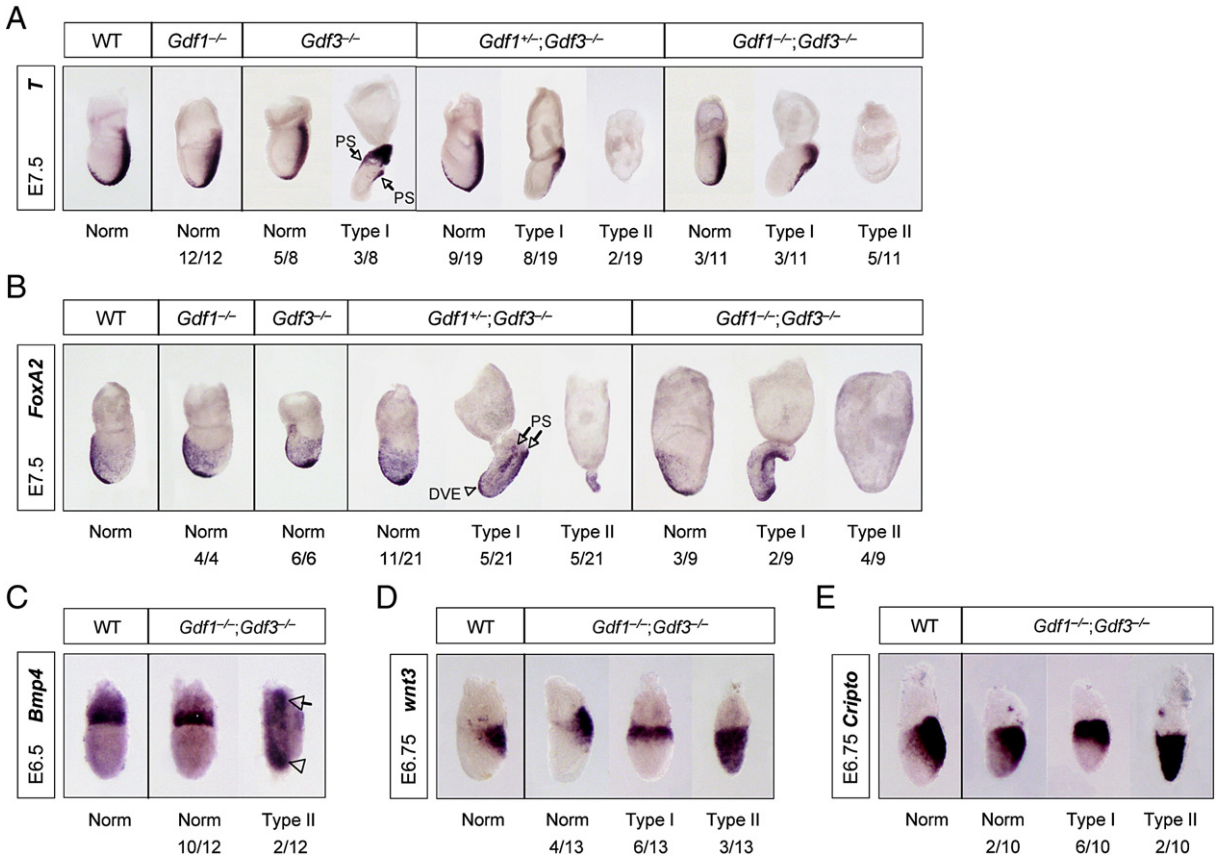

Fig. 6. Deletion of *Gdf1* and *Gdf3* affects mesoderm formation. (A) Expression of *T* in the primitive streak and axial mesoderm of E7.5 wild type, *Gdf1*$^{-/-}$ and *Gdf3*$^{-/-}$ single mutants, and *Gdf1*$^{+/-}$;*Gdf3*$^{-/-}$ and *Gdf1*$^{-/-}$;*Gdf3*$^{-/-}$ compound mutant embryos. Several embryos of the same genotype are shown when variable phenotypes occurred. Phenotypes were grouped into different classes (normal, type I and type II) as explained in the text. The frequency of each phenotype within a given genotype is indicated. One type I embryo has a double axis, as denoted by two primitive streaks (arrows). PS, primitive streak. (B) Expression of *FoxA2* in the anterior primitive streak and axial mesoderm of E7.5 wild type, *Gdf1*$^{-/-}$ and *Gdf3*$^{-/-}$ single mutants, and *Gdf1*$^{+/-}$;*Gdf3*$^{-/-}$ and *Gdf1*$^{-/-}$;*Gdf3*$^{-/-}$ compound mutant embryos. Two primitive streaks (arrows) and distal visceral endoderm (arrowhead) are indicated in one type I embryo. DVE, distal visceral endoderm; PS, primitive streak. (C) Expression of *Bmp4* in E6.5 wild type and *Gdf1*$^{-/-}$;*Gdf3*$^{-/-}$ compound mutants. *Bmp4* is normally expressed in the extra-embryonic ectoderm in wild type embryos (norm), but ectopic patches of *Bmp4* expression was found distally (arrowhead), as well as proximally (arrow), in a subset of *Gdf1*$^{-/-}$;*Gdf3*$^{-/-}$ mutants (type II). (D) Expression of *wnt3* in the epiblast of E6.75 wild type and *Gdf1*$^{-/-}$;*Gdf3*$^{-/-}$ compound mutants. *Wnt3* is normally restricted to the posterior side of the epiblast in wild type embryos (norm), but was found to be expressed uniformly in the proximal embryonic ectoderm (Type I), or throughout the epiblast (Type II) in affected compound mutant embryos. (E) Expression of *Cripto* in the epiblast of E6.75 wild type and *Gdf1*$^{-/-}$;*Gdf3*$^{-/-}$ compound mutants. *Cripto* has a similar expression pattern as *Wnt3* and is restricted to the posterior side of the epiblast in wild type embryos (norm), but was also found uniformly expressed in the proximal embryonic ectoderm (Type I), or else found throughout the epiblast (Type II) in affected compound mutant embryos.

as type I. A fraction of these embryos (41%, $n=17$) displayed two primitive streaks, indicating formation of a secondary axis (see for example type I *Gdf3*$^{-/-}$ mutant in Fig. 6A or type I *Gdf1*$^{+/-}$;*Gdf3*$^{-/-}$ mutant in Fig. 6B). In these embryos, expression of *FoxA2* at E7.5 revealed abnormal anterior primitive streak and axial mesoderm (Fig. 6B). We also found *FoxA2* expression in distal visceral endoderm in these embryos, supporting the relationship between type I phenotypes found at different stages. Note that it is sometimes difficult to distinguish AVE from axial mesoderm using *FoxA2* at this stage, as both these cell types locate to the anterior side of the embryo. A second set of E7.5 mutant embryos was more severely affected (herein referred to as type II), in which neither *T* nor *FoxA2* expression could be detected (Figs. 6A and B), indicating a total lack of mesoderm. Weak *FoxA2* staining was observed in a small cell mass outside the yolk sac in a proportion of these embryos (Fig. 6B). Collectively, the analysis of *FoxA2* and *T* expression suggests that mutations in *Gdf1* can potentiate the defects in mesoderm formation found in *Gdf3* mutant embryos.

Finally, to further characterize the effects of GDF1 and GDF3 on mesoderm formation, we investigated the expression of *Bmp4*, *Wnt3* and *Cripto* in wild type and *Gdf1*$^{-/-}$;*Gdf3*$^{-/-}$ embryos at E6.5 and E6.75 (Figs. 6C to E). Together with *Nodal*, these three genes constitute a feed-forward signaling loop that mediates reciprocal interactions between the epiblast and extra-embryonic ectoderm that are essential for mesoderm formation (Ang and Constam, 2004). In this signaling circuit, epiblast-derived Nodal maintains *Bmp4* expression in extra-embryonic ectoderm (Brennan et al., 2001; Mesnard et al., 2006), which in turn acts back on the epiblast to increase expression of *Wnt3* (Ben-Haim et al., 2006), a known positive regulator of *Nodal* and *Cripto* (Ben-Haim et al., 2006; Liu et al., 1999; Morkel et al., 2003). We found that *Bmp4* expression was restricted to the extra-embryonic ectoderm in wild type and the majority of mutant embryos at E6.5 (Fig. 6C). However, patches of ectopic *Bmp4* expression, extending into regions normally containing embryonic ectoderm, were observed in a few mutants (referred to as type II in Fig. 6C). *Wnt3* expression was restricted to the posterior epiblast in wild type and one third of mutant embryos at E6.75 (Fig. 6D). In the remaining mutants, *Wnt3* transcripts were abnormally expressed, either uniformly across the proximal epiblast or throughout the whole embryonic ectoderm (referred to as type I and II in Fig. 6D, respectively). A similar pattern was observed for *Cripto* expression, which like that of *Wnt3* is also normally limited to the posterior epiblast. Affected embryos (80%) displayed *Cripto* expression either across the proximal epiblast or throughout the whole embryonic ectoderm (Fig. 6E). Together, these results suggest that although the *Nodal–Bmp4–Wnt3–Cripto* signaling loop between the epiblast and extra-embryonic ectoderm appears to be functional in *Gdf1*$^{-/-}$;*Gdf3*$^{-/-}$ embryos, this would seem to be deregulated, taking place across the proximal epiblast, or throughout the entire epiblast of the most affected embryos.

The synergistic interaction between *Gdf1* and *Gdf3* during the early embryonic development of the mouse can be summarized in quantitative terms as follows. Among *Gdf3*$^{-/-}$ single mutants, we found 15% type I embryos at E7.5 but only one (out of 26) type II (Table 1). In contrast, type II embryos were found in 18% and 47% of E7.5 *Gdf1*$^{+/-}$;*Gdf3*$^{-/-}$ and *Gdf1*$^{-/-}$;*Gdf3*$^{-/-}$ compound mutants, respectively (Table 1), indicating a progressive, dose-dependent enhancement of the incidence of this more severe phenotype. Together, our studies reveal that 28% of *Gdf3*$^{-/-}$ mutants ($n=44$), 40% of *Gdf1*$^{+/-}$;*Gdf3*$^{-/-}$ mutants ($n=74$), and 74% of *Gdf1*$^{-/-}$;*Gdf3*$^{-/-}$ mutants ($n=82$) displayed patterning defects between E6.25 and E8.5, supporting the notion that *Gdf1* and *Gdf3* genetically interact during early embryonic development.

Table 1
Summary of the incidence of type I and type II phenotypes among *Gdf1;Gdf3* compound mutant embryos analyzed by whole-mount *in situ* hybridization at E6.5–E6.75 and E7.5

	E6.5–6.75			E7.5		
	Normal (%)	Type I (%)	Type II (%)	Normal (%)	Type I (%)	Type II (%)
Gdf1$^{+/+}$;*Gdf3*$^{-/-}$	53	31	15	81	15	4
Gdf1$^{+/-}$;*Gdf3*$^{-/-}$	55	30	15	52	30	18
Gdf1$^{-/-}$;*Gdf3*$^{-/-}$	24	38	38	26	26	47

Discussion

GDF1 and GDF3 cooperate during early embryonic development

In this study, we demonstrate that GDF1 and GDF3 share signaling mechanisms and functions with each other and with Nodal, and display synergistic interactions during early embryonic development. Throughout our analysis, we have distinguished two types of phenotypes in affected embryos based on their severity. At E6.5, the less severe phenotype – which we have called type I – involved defects in the anterior migration of AVE, ectopic expression of *T* in the proximal part of the embryonic ectoderm, and abnormal expression of *Nodal*, *Wnt3* and *Cripto* across the proximal epiblast. The most severe phenotype – termed type II – included total absence of AVE, ectopic expression of *T* throughout the whole epiblast, abnormal *Nodal* expression in the visceral endoderm, and expression of *Wnt3* and *Cripto* throughout the embryonic ectoderm. At E7.5, embryos showing the less severe, type I phenotype displayed a constriction at the extra-embryonic/embryonic junction, showed defects in primitive streak elongation – but were still able to form mesoderm, and abnormal expression of *Otx2* in the distal epiblast and of *FoxA2* in distal visceral endoderm. The most severely affected, type II embryos at this stage had relatively normal extra-embryonic tissues but no or very small and disorganized embryo proper, showed no *T* or *FoxA2* expression – indicating a total lack of mesoderm, and lacked expression of *Otx2*. Although this classification was primarily chosen to simplify the presentation of a complex set of phenotypes obtained with different probes at different ages, we believe that there is indeed a relationship among the different phenotypes observed within either type I or type II embryos at the ages examined. In support of this, we note the similarity between the

type II phenotypes described here and those previously observed in *Smad2*$^{-/-}$ mutant embryos, which lack epiblast derivatives and contain an internal cell population comprised by a loose mesenchymal cell mass (Waldrip et al., 1998). Similar to type II *Gdf1*$^{-/-}$;*Gdf3*$^{-/-}$ embryos, *Smad2*$^{-/-}$ mutants display ectopic expression of *Wnt3* and *Cripto* throughout the embryonic ectoderm and, intriguingly, differ from *Nodal*$^{-/-}$ mutants, in which *Wnt3* and *Cripto* expression is totally absent (Brennan et al., 2001). This function of Nodal is believed to be mediated by Smad2-independent pathways, possibly by Smad3, which is highly expressed in extra-embryonic ectoderm but low in the embryo proper (Tremblay et al., 2000). Nodal and GDF1/GDF3 would thus appear to differ in their requirement for induction and maintenance of the reciprocal interactions between the epiblast and the extra-embryonic ectoderm that are required for appropriate *Wnt3* and *Cripto* expression in the epiblast. This may be due to a differential ability to pattern extra-embryonic tissues and maintain *Bmp4* expression, which is essentially absent in *Nodal*$^{-/-}$ mutants at E6.5 but present in both *Gdf1*$^{-/-}$;*Gdf3*$^{-/-}$ and *Smad2*$^{-/-}$ mutants (Brennan et al., 2001). The reason why GDF1 and GDF3 do not overlap with Nodal in this function is unclear, but may be related to an inability of GDF1 and GDF3 to act across the distances required to reach extra-embryonic ectoderm.

It has previously been suggested that Nodal signals from the epiblast to the extra-embryonic visceral endoderm to induce distal visceral endoderm, which subsequently migrates to the prospective anterior side of the epiblast to form the AVE. Extra-embryonic ectoderm inhibits the formation of the AVE, which may explain why distal visceral endoderm is induced at the apex of the epiblast (Rodriguez et al., 2005). The mechanism regulating migration of these cells from the distal to the anterior side of the epiblast is less clear, although it seems to involve Otx2, Wnt, and Nodal signaling (Kimura et al., 2000; Kimura-Yoshida et al., 2005; Yamamoto et al., 2001). In this study, we show that GDF1 and GDF3 cooperate in the induction and migration of the AVE. In type I embryos, the distal visceral endoderm remains at the apex of the epiblast and, later in development, elongation of the primitive streak is impaired. This observations support the hypothesis that AVE migration converts the proximal–distal axis into an anterior–posterior axis (Beddington and Robertson, 1999). On the other hand, type II embryos lack AVE and mesoderm altogether. These two classes of phenotypes have also been observed by Chen et al. in their analysis of *Gdf3*$^{-/-}$ single mutants (Chen et al., 2006). Together with previous work, our present results indicate that Nodal, GDF1, and GDF3 share common downstream signaling components and display partial overlap in their functions, allowing functional redundancy and complementarity during establishment of an anterior–posterior identity.

Deletion of Gdf1 and Gdf3 affects mesoderm formation

Induction of mesoderm and formation of the primitive streak is thought to depend on several signals derived from both embryonic and extra-embryonic structures. *Nodal* and *Wnt3* expression become restricted to the posterior side of the epiblast by the secretion of multiple inhibitory molecules from the AVE. These signals act together with BMP4, which is secreted from the extra-embryonic ectoderm, to induce mesoderm at the proximal/posterior side of the epiblast (Winnier et al., 1995). We found that type I *Gdf1*$^{-/-}$;*Gdf3*$^{-/-}$ embryos appear to be able to induce mesoderm in a relatively normal manner, although not necessarily at the posterior side of the proximal epiblast. In these embryos, which lack an anterior–posterior identity, expression of *Nodal* and *Wnt3* was not restricted to the proximal/posterior side of the epiblast, which may explain the altered position of mesoderm formation. Subsequently, the elongation of the primitive streak may be inhibited by the distal visceral endoderm that failed to migrate to the anterior side. As indicated above, however, type II embryos resemble Smad2$^{-/-}$ mutants, which lack AVE and fail to form mesoderm (Brennan et al., 2001; Waldrip et al., 1998). We found ectopic expression of *T* – a mesodermal marker – in these embryos at pre-gastrulation stages, although this expression was transient and *T* transcripts were absent altogether at later gastrulation stages. Whether GDF1 and GDF3 affect mesoderm induction directly or secondarily to changes in Nodal signaling or AVE formation is unclear at present. A possibility indicated by our results showing synergy between Nodal and GDF1/GDF3 in reporter gene assays is that lack of GDF1 and GDF3 may compromise the ability of Nodal to signal efficiently in the epiblast. Alternatively, or in addition, reciprocal interactions between the epiblast and the extra-embryonic ectoderm could also have contributed to this phenotype. It is thus possible that ectopic expression of *Bmp4* observed in type II *Gdf1*$^{-/-}$;*Gdf3*$^{-/-}$ mutants leads to ectopic expression of *Wnt3*, and subsequently *Cripto*, throughout the epiblast. This cascade of events may underlay the premature but transient mesodermal fate found in the epiblast of these mutants.

GDF1 and GDF3 as the functional mammalian homologs of Vg1

The cooperativity displayed by GDF1 and GDF3 during AVE formation and mesoderm induction is highly reminiscent of the functions attributed to Vg1, which has been suggested to control mesoderm induction during early *Xenopus* and chick embryogenesis (Birsoy et al., 2005; Kessler and Melton, 1995; Skromne and Stern, 2001; Thomsen and Melton, 1993). This suggests that GDF1 and GDF3 may together represent a functional mammalian counterpart of Vg1. Later during development, Vg1 has been proposed to regulate left–right patterning in a similar manner as does GDF1 in the mouse (Hyatt and Yost, 1998; Rankin et al., 2000). We did not find any left–right patterning defects in *Gdf3*$^{-/-}$ mutants, so this function may be restricted to GDF1. The fact that approximately 25% of *Gdf1*$^{-/-}$;*Gdf3*$^{-/-}$ compound mutants developed normally suggests that there must be another ligand – most likely Nodal – that can occasionally compensate for the absence of GDF1 and GDF3. It has previously been suggested that *Gdf3* mutant embryos display variable and partial penetrant phenotypes due in part to abnormal expression of *Nodal* (Chen et al., 2006). Likewise, Vg1 has been proposed to act upstream of *Nodal*

during initiation of the primitive streak in chick embryos (Skromne and Stern, 2001). We found that the expression of *Nodal* was often lower in double mutant embryos, indicating that GDF1 and GDF3 may act upstream of Nodal. It has previously been shown that Nodal can partially regulate its own expression by an intronic enhancer, which is activated by a complex of phosphorylated Smad2 or 3 and the transcription factor FoxH1 (Norris et al., 2002). Given that GDF1 and GDF3 can also activate Smad2 and 3, it is possible that these ligands can also contribute to fine-tuning *Nodal* expression.

Redundancy and cooperativity in the TGF-β superfamily

Different scenarios can be envisioned to explain the observed cooperativity among TGF-β superfamily ligands during early embryonic development. Redundant functions may help to ensure that a critical event does not fail to take place, a property of signaling networks that it is sometimes referred to as robustness. If Nodal, GDF1 and GDF3 act in parallel during formation of the AVE, mutations in any one of the alleles encoding any of these ligands is less likely to alter the outcome of their common function. This type of redundancy may be particularly important for the fidelity of inter-cellular signaling in tissues undergoing rapid morphological variations due to growth or cellular movements, in which achievement of certain strength may be critical for a given signal to reach its cellular target.

Previous studies have suggested that GDF1 and GDF3 require Cripto for signaling (Chen et al., 2006; Cheng et al., 2003). However, those results were obtained using chimeric constructs carrying Activin or BMP pro-domains. In this study, we show that native GDF1 and GDF3 can indeed signal in a Cripto-dependent manner when co-expressed with Furin. Studies in *Furin*$^{-/-}$;*Spc4*$^{-/-}$ compound mutant mice have revealed a critical role for pro-protein convertases in AVE and mesendoderm formation by promoting cleavage and activation of Nodal (Beck et al., 2002). Specifically, soluble Furin and Spc4 derived from the extra-embryonic ectoderm were proposed to control cleavage of Nodal in the epiblast. Since, as shown here, Furin can also process GDF1 and GDF3, it is possible that insufficient cleavage of these ligands may also contribute to the defects found in *Furin*$^{-/-}$;*Spc4*$^{-/-}$ mutants. The fact that other TGF-β superfamily ligands were readily processed in HepG2 cells without Furin overexpression suggests that different TGF-β precursors may normally be cleaved by different pro-protein convertases. In the future, it will be critical to determine the efficiency by which convertases process individual ligands, since this may represent another important level of regulation for the activities of TGF-β superfamily ligands.

Co-expression of either GDF1 or GDF3 with Nodal uncovered the activity of native GDF1 and GDF3 proteins – which otherwise proved to be inactive on their own in reporter assays in HepG2 cells – by potentiating Nodal activity in a synergistic manner. It is possible that this has relevance for the function of these molecules in vivo, as GDF1 and GDF3 appear to be co-expressed with Nodal in many structures of the early mouse embryo. However, it is unlikely that Nodal co-expression is an absolute requirement for the actions of these two ligands, since both GDF1 and GDF3 are expressed in many regions without Nodal, such as adult nervous system and adipose tissue, respectively (Lee, 1991; McPherron and Lee, 1993). On the other hand, it is possible that Nodal co-expression facilitates processing or secretion of GDF1 and GDF3, perhaps by inducing the expression of pro-protein convertases. In support of this notion, TGF-β1 has been shown to upregulate the expression of Furin through Smad2 signaling mechanisms (Blanchette et al., 1997; Blanchette et al., 2001). Alternatively, or in addition, Nodal may form heterodimeric complexes with GDF1 and GDF3 which may have increased signaling efficacy compared to Nodal homodimers. In *Drosophila*, heterodimers of BMP-like ligands Dpp and Scw show enhanced signaling and facilitated transport compared to homodimers (Shimmi et al., 2005). Moreover, GDF3 has been shown to form heterodimeric complexes with BMP4, thereby inhibiting BMP4 signaling (Levine and Brivanlou, 2006). Several other TGF-β superfamily ligands have previously been shown to form heterodimeric complexes resulting in either inhibition or potentiation of signaling, including Activin AB, Inhibin A, Inhibin B, Nodal/BMP7, Derriere/Xnr2, Derriere/BMP4, and BMP2/BMP7 (Eimon and Harland, 2002; Israel et al., 1996; Ling et al., 1986; Yeo and Whitman, 2001). However, with the exception of Inhibins and Activin AB, there is no evidence as yet for the existence of heterodimeric complexes of endogenously expressed ligands, and so the possible physiological importance of these complexes for mouse development remains to be established.

The molecular mechanisms underlying the establishment of the different embryonic axes during metazoan development have been the subject of intense study. In the mouse, the variety of phenotypes uncovered by targeted deletion of genes encoding ligands, receptors, co-receptors and intracellular mediators of the TGF-β superfamily reflect the complexity of this signaling network. Interestingly, the strongest phenotypes have been found after deletion of the main intracellular mediators of Nodal, TGF-β and Activin signaling, namely in *Smad2*$^{-/-}$;*Smad3*$^{-/-}$ and *Smad4*$^{-/-}$ mutant embryos, which lead to arrested embryonic development before gastrulation (Dunn et al., 2004; Sirard et al., 1998; Yang et al., 1998). Our present and previous results indicate that *Gdf1*, *Gdf3* and *Nodal* cooperate to form a signaling network in which they display partially redundant functions, and suggest that simultaneous deletion of these three genes may resemble the deficits observed in *Smad2*$^{-/-}$;*Smad3*$^{-/-}$ mutant embryos.

Experimental procedures

Mouse strains and PCR primers

Gdf1 mutant mice used in this study were generated by Se-Jin Lee and colleagues (Rankin et al., 2000). *Gdf3* mutant mice were generated from ES cells obtained from The Wellcome Trust Sanger Institute carrying a gene trap in the single intron of the *Gdf3* gene (pGT01xr clone AD0857). All experiments shown were performed in a Sv129;C57BL/6 hybrid strain, although we also generated *Gdf3* mutant mice in a Sv129OlaHsd inbred background, which showed similar survival rates. Littermates were used as controls in all experiments. Embryos were genotyped by PCR using the following sets of primers: *Gdf1* wild type allele 5′-TCGAAGAAGAGCACGGAGAT-3′ and 5′-ATGTGAGCTTCCGT-

GAGGTG-3′, *Gdf1* targeted allele 5′-CCACTGCAGCCTGTGGGCGC-3′ and 5′-GGAAGACAATAGCAGGCATGCTGG-3, *Gdf3* wild type allele 5′-CACTGCATGGATCTCCGAAT-3′ and 5′-GGGAGCTCAAACCCAGAAC-3′, *Gdf3* targeted allele 5′-ATCCTCTGCATGGTCAGGTC-3′ and 5′-CGTGG-CCTGATTCATTCC-3′. RT–PCR for *Gdf3* was performed with the following set of primers: 5′-CGTGAAGGAGCTGGGTGTT-3′ and 5′-CCTGCATGA-AAGCATAATTGGA-3′. Animal protocols were approved by Stockholms Norra djurförsöksetiska nämnd and were in accord with the ethical guidelines of the Karolinska Institute.

Receptor reconstitution experiments

A DNA fragment encoding the mature region of mouse GDF3 was fused downstream to a *Xenopus* Activin B pro-domain and a hemagglutinin (HA)-tag, such that, after processing, the HA-tag remained at the N-terminus of mature GDF3. This construct was cloned into a pCDNA3.1 vector backbone for expression in mammalian cells. GDF3 was processed and secreted as a mature protein of the expected size when expressed from this construct (data not shown). The chimeric type I receptor ALK4 L45-ALK3 (ALK4/3) was generated by substituting Asn269, Asp271, Asn272, and Thr274 of ALK4 with Ile269, Gly271, Thr272, and Ser274, respectively, by site-directed mutagenesis. Receptor reconstitution and reporter gene experiments were performed in R4-2 and HepG2 cells cultured in 24-well plates, as previously described (Reissmann et al., 2001). The amounts of plasmid DNA transfected into cells (per 3 wells) were as follows: 10 ng for type I receptors; 100 ng for chimeric type I receptors; 2 ng for type II receptors; 30 ng for Cripto; 600 ng for Furin; and 50, 200, or 800 ng for ligands (800 ng was used if nothing else was indicated in the figure legend).

Whole-mount in situ hybridization

Whole-mount *in situ* hybridization was performed according to standard protocols using RNA-probes labeled with digoxigenin (DIG RNA Labeling Kit, Roche). Probes were transcribed from plasmids encoding *Lefty1* (Oulad-Abdelghani et al., 1998), *Nodal* (Varlet et al., 1997), *T* (Herrmann, 1991), *Otx2* (Matsuo et al., 1995), *Cripto* (Shen et al., 1997), *Bmp4* (Jones et al., 1991), *wnt3* (Roelink et al., 1990), and *FoxA2* (Sasaki and Hogan, 1993).

Acknowledgments

We are grateful to S.-J. Lee for providing *Gdf1* mutant mice; The Wellcome Trust Sanger Institute for providing the *Gdf3* gene trap ES cell-line; E.M. De Robertis, P.P. Tam, M.M. Shen, I. Matsuo, A.-H. Brivanlou, D.B. Constam, B.G. Herrmann, B.L. Hogan, D.S. Kessler, H. Hamada, S.-J. Lee, A.F. Schier, and S.L. Ang for providing plasmids; and Carolyn Marks for comments on the manuscript. This work was supported by grants from the Swedish Foundation for Strategic Research, Swedish Cancer Society, the Swedish Research Council, and the Karolinska Institute.

References

Andersson, O., Reissmann, E., Ibanez, C.F., 2006a. Growth differentiation factor 11 signals through the transforming growth factor-beta receptor ALK5 to regionalize the anterior–posterior axis. EMBO Rep. 7, 831–837.

Andersson, O., Reissmann, E., Jornvall, H., Ibanez, C.F., 2006b. Synergistic interaction between Gdf1 and Nodal during anterior axis development. Dev. Biol. 293, 370–381.

Ang, S.L., Constam, D.B., 2004. A gene network establishing polarity in the early mouse embryo. Semin. Cell Dev. Biol. 15, 555–561.

Beck, S., Le Good, J.A., Guzman, M., Ben Haim, N., Roy, K., Beermann, F., Constam, D.B., 2002. Extraembryonic proteases regulate Nodal signalling during gastrulation. Nat. Cell Biol. 4, 981–985.

Beddington, R.S., Robertson, E.J., 1999. Axis development and early asymmetry in mammals. Cell 96, 195–209.

Ben-Haim, N., Lu, C., Guzman-Ayala, M., Pescatore, L., Mesnard, D., Bischofberger, M., Naef, F., Robertson, E.J., Constam, D.B., 2006. The nodal precursor acting via activin receptors induces mesoderm by maintaining a source of its convertases and BMP4. Dev. Cell 11, 313–323.

Birsoy, B., Berg, L., Williams, P.H., Smith, J.C., Wylie, C.C., Christian, J.L., Heasman, J., 2005. XPACE4 is a localized pro-protein convertase required for mesoderm induction and the cleavage of specific TGFbeta proteins in *Xenopus* development. Development 132, 591–602.

Birsoy, B., Kofron, M., Schaible, K., Wylie, C., Heasman, J., 2006. Vg1 is an essential signaling molecule in *Xenopus* development. Development 133, 15–20.

Blanchette, F., Day, R., Dong, W., Laprise, M.H., Dubois, C.M., 1997. TGFbeta1 regulates gene expression of its own converting enzyme furin. J. Clin. Invest. 99, 1974–1983.

Blanchette, F., Rudd, P., Grondin, F., Attisano, L., Dubois, C.M., 2001. Involvement of Smads in TGFbeta1-induced furin (fur) transcription. J. Cell. Physiol. 188, 264–273.

Brennan, J., Lu, C.C., Norris, D.P., Rodriguez, T.A., Beddington, R.S., Robertson, E.J., 2001. Nodal signalling in the epiblast patterns the early mouse embryo. Nature 411, 965–969.

Chen, Y.G., Hata, A., Lo, R.S., Wotton, D., Shi, Y., Pavletich, N., Massague, J., 1998. Determinants of specificity in TGF-beta signal transduction. Genes Dev.. 12, 2144–2152.

Chen, C., Ware, S.M., Sato, A., Houston-Hawkins, D.E., Habas, R., Matzuk, M.M., Shen, M.M., Brown, C.W., 2006. The Vg1-related protein Gdf3 acts in a Nodal signaling pathway in the pre-gastrulation mouse embryo. Development 133, 319–329.

Cheng, S.K., Olale, F., Bennett, J.T., Brivanlou, A.H., Schier, A.F., 2003. EGF-CFC proteins are essential coreceptors for the TGF-beta signals Vg1 and GDF1. Genes Dev. 17, 31–36.

Cheng, S.K., Olale, F., Brivanlou, A.H., Schier, A.F., 2004. Lefty blocks a subset of TGFbeta signals by antagonizing EGF-CFC coreceptors. PLoS Biol. 2, E30.

Dennler, S., Itoh, S., Vivien, D., ten Dijke, P., Huet, S., Gauthier, J.M., 1998. Direct binding of Smad3 and Smad4 to critical TGF beta-inducible elements in the promoter of human plasminogen activator inhibitor-type 1 gene. EMBO. J. 17, 3091–3100.

Ding, J., Yang, L., Yan, Y.T., Chen, A., Desai, N., Wynshaw-Boris, A., Shen, M.M., 1998. Cripto is required for correct orientation of the anterior–posterior axis in the mouse embryo. Nature 395, 702–707.

Dunn, N.R., Vincent, S.D., Oxburgh, L., Robertson, E.J., Bikoff, E.K., 2004. Combinatorial activities of Smad2 and Smad3 regulate mesoderm formation and patterning in the mouse embryo. Development 131, 1717–1728.

Eimon, P.M., Harland, R.M., 2002. Effects of heterodimerization and proteolytic processing on Derriere and Nodal activity: implications for mesoderm induction in *Xenopus*. Development 129, 3089–3103.

Hata, A., Seoane, J., Lagna, G., Montalvo, E., Hemmati-Brivanlou, A., Massague, J., 2000. OAZ uses distinct DNA- and protein-binding zinc fingers in separate BMP-Smad and Olf signaling pathways. Cell 100, 229–240.

Heasman, J., 2006. Patterning the early *Xenopus* embryo. Development 133, 1205–1217.

Herrmann, B.G., 1991. Expression pattern of the Brachyury gene in whole-mount TWis/TWis mutant embryos. Development 113, 913–917.

Hyatt, B.A., Yost, H.J., 1998. The left–right coordinator: the role of Vg1 in organizing left–right axis formation. Cell 93, 37–46.

Israel, D.I., Nove, J., Kerns, K.M., Kaufman, R.J., Rosen, V., Cox, K.A., Wozney, J.M., 1996. Heterodimeric bone morphogenetic proteins show enhanced activity in vitro and in vivo. Growth Factors 13, 291–300.

Jones, C.M., Lyons, K.M., Hogan, B.L., 1991. Involvement of bone morphogenetic protein-4 (BMP-4) and Vgr-1 in morphogenesis and neurogenesis in the mouse. Development 111, 531–542.

Joseph, E.M., Melton, D.A., 1998. Mutant Vg1 ligands disrupt endoderm and mesoderm formation in *Xenopus* embryos. Development 125, 2677–2685.

Kessler, D.S., Melton, D.A., 1995. Induction of dorsal mesoderm by soluble, mature Vg1 protein. Development 121, 2155–2164.

Kimura, C., Yoshinaga, K., Tian, E., Suzuki, M., Aizawa, S., Matsuo, I., 2000. Visceral endoderm mediates forebrain development by suppressing posteriorizing signals. Dev. Biol. 225, 304–321.

Kimura-Yoshida, C., Nakano, H., Okamura, D., Nakao, K., Yonemura, S., Belo, J.A., Aizawa, S., Matsui, Y., Matsuo, I., 2005. Canonical Wnt signaling and its antagonist regulate anterior–posterior axis polarization by guiding cell migration in mouse visceral endoderm. Dev. Cell 9, 639–650.

Lee, S.J., 1991. Expression of growth/differentiation factor 1 in the nervous system: conservation of a bicistronic structure. Proc. Natl. Acad. Sci. U. S. A. 88, 4250–4254.

Levine, A.J., Brivanlou, A.H., 2006. GDF3, a BMP inhibitor, regulates cell fate in stem cells and early embryos. Development 133, 209–216.

Ling, N., Ying, S.Y., Ueno, N., Shimasaki, S., Esch, F., Hotta, M., Guillemin, R., 1986. Pituitary FSH is released by a heterodimer of the beta-subunits from the two forms of inhibin. Nature 321, 779–782.

Liu, P., Wakamiya, M., Shea, M.J., Albrecht, U., Behringer, R.R., Bradley, A., 1999. Requirement for Wnt3 in vertebrate axis formation. Nat. Genet. 22, 361–365.

Lowe, L.A., Yamada, S., Kuehn, M.R., 2001. Genetic dissection of nodal function in patterning the mouse embryo. Development 128, 1831–1843.

Matsuo, I., Kuratani, S., Kimura, C., Takeda, N., Aizawa, S., 1995. Mouse Otx2 functions in the formation and patterning of rostral head. Genes Dev. 9, 2646–2658.

McPherron, A.C., Lee, S.J., 1993. GDF-3 and GDF-9: two new members of the transforming growth factor-beta superfamily containing a novel pattern of cysteines. J. Biol. Chem. 268, 3444–3449.

Mesnard, D., Guzman-Ayala, M., Constam, D.B., 2006. Nodal specifies embryonic visceral endoderm and sustains pluripotent cells in the epiblast before overt axial patterning. Development 133, 2497–2505.

Morkel, M., Huelsken, J., Wakamiya, M., Ding, J., van de Wetering, M., Clevers, H., Taketo, M.M., Behringer, R.R., Shen, M.M., Birchmeier, W., 2003. Beta-catenin regulates Cripto- and Wnt3-dependent gene expression programs in mouse axis and mesoderm formation. Development 130, 6283–6294.

Norris, D.P., Brennan, J., Bikoff, E.K., Robertson, E.J., 2002. The Foxh1-dependent autoregulatory enhancer controls the level of Nodal signals in the mouse embryo. Development 129, 3455–3468.

Oulad-Abdelghani, M., Chazaud, C., Bouillet, P., Mattei, M.G., Dolle, P., Chambon, P., 1998. Stra3/lefty, a retinoic acid-inducible novel member of the transforming growth factor-beta superfamily. Int. J. Dev. Biol. 42, 23–32.

Persson, U., Izumi, H., Souchelnytskyi, S., Itoh, S., Grimsby, S., Engstrom, U., Heldin, C.H., Funa, K., ten Dijke, P., 1998. The L45 loop in type I receptors for TGF-beta family members is a critical determinant in specifying Smad isoform activation. FEBS Lett. 434, 83–87.

Rankin, C.T., Bunton, T., Lawler, A.M., Lee, S.J., 2000. Regulation of left–right patterning in mice by growth/differentiation factor-1. Nat. Genet. 24, 262–265.

Reissmann, E., Jornvall, H., Blokzijl, A., Andersson, O., Chang, C., Minchiotti, G., Persico, M.G., Ibanez, C.F., Brivanlou, A.H., 2001. The orphan receptor ALK7 and the Activin receptor ALK4 mediate signaling by Nodal proteins during vertebrate development. Genes Dev. 15, 2010–2022.

Rodriguez, T.A., Srinivas, S., Clements, M.P., Smith, J.C., Beddington, R.S., 2005. Induction and migration of the anterior visceral endoderm is regulated by the extra-embryonic ectoderm. Development 132, 2513–2520.

Roelink, H., Wagenaar, E., Lopes da Silva, S., Nusse, R., 1990. *Wnt-3*, a gene activated by proviral insertion in mouse mammary tumors, is homologous to int-1/Wnt-1 and is normally expressed in mouse embryos and adult brain. Proc. Natl. Acad. Sci. U. S. A. 87, 4519–4523.

Rossant, J., Tam, P.P., 2004. Emerging asymmetry and embryonic patterning in early mouse development. Dev. Cell 7, 155–164.

Sasaki, H., Hogan, B.L., 1993. Differential expression of multiple fork head related genes during gastrulation and axial pattern formation in the mouse embryo. Development 118, 47–59.

Shen, M.M., 2007. Nodal signaling: developmental roles and regulation. Development 134 (6), 1023–1034.

Shen, M.M., Wang, H., Leder, P., 1997. A differential display strategy identifies *Cryptic*, a novel EGF-related gene expressed in the axial and lateral mesoderm during mouse gastrulation. Development 124, 429–442.

Shi, Y., Massague, J., 2003. Mechanisms of TGF-beta signaling from cell membrane to the nucleus. Cell 113 (6), 685–700.

Shimmi, O., Umulis, D., Othmer, H., O'Connor, M.B., 2005. Facilitated transport of a Dpp/Scw heterodimer by Sog/Tsg leads to robust patterning of the *Drosophila* blastoderm embryo. Cell 120, 873–886.

Sirard, C., de la Pompa, J.L., Elia, A., Itie, A., Mirtsos, C., Cheung, A., Hahn, S., Wakeham, A., Schwartz, L., Kern, S.E., Rossant, J., Mak, T.W., 1998. The tumor suppressor gene *Smad4/Dpc4* is required for gastrulation and later for anterior development of the mouse embryo. Genes Dev. 12, 107–119.

Skromne, I., Stern, C.D., 2001. Interactions between Wnt and Vg1 signalling pathways initiate primitive streak formation in the chick embryo. Development 128, 2915–2927.

Sossin, W.S., 2006. Tracing the evolution and function of the Trk superfamily of receptor tyrosine kinases. Brain Behav. Evol. 68, 145–156.

Takaoka, K., Yamamoto, M., Shiratori, H., Meno, C., Rossant, J., Saijoh, Y., Hamada, H., 2006. The mouse embryo autonomously acquires anterior–posterior polarity at implantation. Dev. Cell 10, 451–459.

Tam, P.P., Loebel, D.A., Tanaka, S.S., 2006. Building the mouse gastrula: signals, asymmetry and lineages. Curr. Opin. Genet. Dev. 16, 419–425.

Thompson, J.D., Higgins, D.G., Gibson, T.J., 1994. CLUSTAL W: improving the sensitivity of progressive multiple sequence alignment through sequence weighting, position-specific gap penalties and weight matrix choice. Nucleic Acids Res. 22, 4673–4680.

Thomsen, G.H., Melton, D.A., 1993. Processed Vg1 protein is an axial mesoderm inducer in *Xenopus*. Cell 74, 433–441.

Tremblay, K.D., Hoodless, P.A., Bikoff, E.K., Robertson, E.J., 2000. Formation of the definitive endoderm in mouse is a Smad2-dependent process. Development 127, 3079–3090.

Varlet, I., Collignon, J., Robertson, E.J., 1997. *nodal* expression in the primitive endoderm is required for specification of the anterior axis during mouse gastrulation. Development 124, 1033–1044.

Vincent, S.D., Dunn, N.R., Hayashi, S., Norris, D.P., Robertson, E.J., 2003. Cell fate decisions within the mouse organizer are governed by graded Nodal signals. Genes Dev. 17, 1646–1662.

Waldrip, W.R., Bikoff, E.K., Hoodless, P.A., Wrana, J.L., Robertson, E.J., 1998. Smad2 signaling in extraembryonic tissues determines anterior–posterior polarity of the early mouse embryo. Cell 92, 797–808.

Wall, N.A., Craig, E.J., Labosky, P.A., Kessler, D.S., 2000. Mesendoderm induction and reversal of left–right pattern by mouse Gdf1, a Vg1-related gene. Dev. Biol. 227, 495–509.

Winnier, G., Blessing, M., Labosky, P.A., Hogan, B.L., 1995. Bone morphogenetic protein-4 is required for mesoderm formation and patterning in the mouse. Genes Dev. 9, 2105–2116.

Yamamoto, M., Meno, C., Sakai, Y., Shiratori, H., Mochida, K., Ikawa, Y., Saijoh, Y., Hamada, H., 2001. The transcription factor FoxH1 (FAST) mediates Nodal signaling during anterior–posterior patterning and node formation in the mouse. Genes Dev. 15, 1242–1256.

Yang, X., Li, C., Xu, X., Deng, C., 1998. The tumor suppressor SMAD4/DPC4 is essential for epiblast proliferation and mesoderm induction in mice. Proc. Natl. Acad. Sci. U. S. A. 95, 3667–3672.

Yeo, C., Whitman, M., 2001. Nodal signals to Smads through Cripto-dependent and Cripto-independent mechanisms. Mol. Cell 7, 949–957.